Design of a switchable driving coil for Magnetic Resonance Wireless Power Transfer

Yelzhas Zhaksylyk, Ulrik Hanke, and Mehdi Azadmehr
Institutt for mikrosystemer - Universitetet i Sørøst-Norge

Accepted version of article in
IEEE PELS Workshop on Emerging Technologies: Wireless Power - WoW 2019

Publisher's version: Zhaksylyk, Y., Hanke, U., & Azadmehr, M. (2019). Design of a switchable driving coil for Magnetic Resonance Wireless Power Transfer. I *2019 IEEE PELS Workshop on Emerging Technologies: Wireless Power Transfer (WoW)* (s. 249-252). IEEE.

DOI: 10.1109/WoW45936.2019.9030674

Design of a switchable driving coil for Magnetic Resonance Wireless Power Transfer

Yelzhas Zhaksylyk, Ulrik Hanke, and Mehdi Azadmehr
Department of Microsystems, University of South-Eastern Norway, Horten, Norway.
Email: yelzhas.zhaksylyk@usn.no.

***Abstract*—This paper presents design and analysis of a switchable inductor suited for active impedance matching in magnetic resonance wireless power transfer systems. The switchable inductor is compact and can be used as both driving coil at the transmitter side and load coil at the receiver side. We first present the concept through design, simulation and measurement of a three loops coil. This model of the switchable coil is used to study the internal couplings between the loops. The coil was fabricated on PCB with inductances between 130-324 nH. In addition, we demonstrate a ten-loop switchable coil for driving a high Q-factor resonance with an almost linear increase in their mutual inductances, which is verified by measurement results.**

***Index Terms*—Impedance matching, inductors, inductive coupling, resonance frequency, selective inductance, wireless power transfer.**

I. Introduction

One of the main challenges of magnetic resonance wireless power transmission (MR WPT) is to maintain high power transfer efficiency throughout different distances between resonator coils. This efficiency instability is due to the impedance mismatch between coils, which can be solved using an effective impedance matching network (IMN) [1]. Moreover, a system with the IMN can be used to power several wireless receiver nodes separately by utilizing a single transceiver [2].

There are many research activities focused on implementation of IMN circuits for WPT. Most of them are based on capacitive circuits where circuits such as capacitor matrices, variable capacitors, or a sequence of predefined capacitors [3]- [6] are used. An alternative, but less common solution is inductive IMN. A recognized solution for WPT is the four-coil magnetic resonance WPT system presented by the MIT in 2007 [7], as shown in Fig. 1. The system consists of two or more high Q-factor resonator coils ($L_T,\ L_R$) which are driven by a low Q-factor coil denoted L_V connected to the power source. The load is also connected to a similar low Q-factor coil also denoted L_V in the figure. The coupling coefficient k_T between transmitting resonant L_T and the driving coil L_V and k_R between the load coil L_V and the receiver resonant L_R can be considered as transformer-based matching networks [1]. An active impedance matching can be achieved by making the driving and load coils L_V tunable. This method referred to as inductive IMN, is discussed and compared to a capacitive IMNs in our previous work [8].

In this paper, we propose a design of the switchable coil L_V, where the optimal inductance value can be selected using switches to improve region of matchable impedances and efficiency [8], [11], [12]. We have fabricated a switchable driving coil L_V and resonating coil L_T on each side of a two-layer PCB with FR4 substrate. Such design offers an easy fabrication process, low cost and compactness.

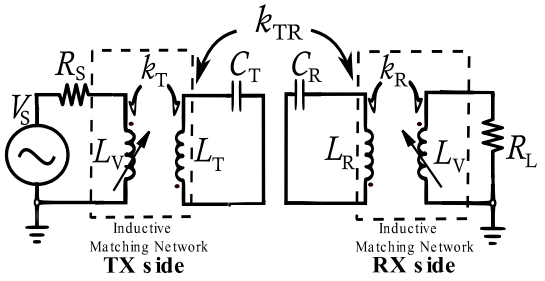

Fig. 1. Equivalent model of four-coil magnetic resonance WPT system.

The paper is organized as follows: In Section II, theoretical analysis of the switchable coil and the working principle of the inductance selectivity is explained. Subsequently, Section III shows the simulation and measurement results used to validate the analytic solution. Furthermore, Section IV discusses the coupling between a switchable driving coil and the resonating spiral coil, while Section V is the conclusion of the study.

II. Design of switchable coil

A. Working principle

One way to realize the switchable driving or load coils L_V in Fig. 1 is by having a set of inductors to choose between. We propose a solution as shown in Fig. 2 where the inductance can be selected via a set of switches. For simplicity of analysis, we chose a three loops coil with different sizes with parameters given in Table I. Here, L_1 is self-inductance for the outer loop, L_2 for middle loop, and L_3 for inner loop. Switches can connect each coil to the power source V_S or ground them for deactivation. In this study, we consider the simplest option when one coil is active, and other two coils are inactive i.e. short-circuited.

B. Self-inductance of the coils

The self-inductance of a planar circular loop is given by Wheeler's formula

$$L_n = 2.25\mu_0 N^2 \frac{d_{avg}}{1+3.55\rho}, \tag{1}$$

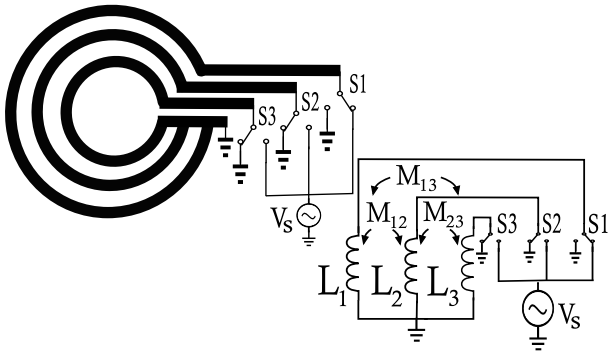

Fig. 2. Design of switchable coil with three loops.

TABLE I
PARAMETERS OF SWITCHABLE INDUCTOR

Parameter	Value	Unit	Description
r_1	9	cm	radius of the loop 1
r_2	7	cm	radius of the loop 2
r_3	5	cm	radius of the loop 3
w	1.2	cm	width of loops
t	35	μm	thickness of the copper

where μ_0 is permeability of free space, N - number of turns, $d_{avg} = 2r_n + w$, $\rho = w/(2r_n + w)$, and the index $n = 1, 2, 3$ represents a loop order [9]. Calculated self-inductances L_n are given in Table II.

C. Analysis of the mutual inductance

Another important parameter is mutual inductance between the loops since they are magnetically coupled to each other, as shown in Fig. 3(a). Here, the outer loop is driven by current I_1, which generates magnetic field B_1 at the center of the circle (at the distance r_1).

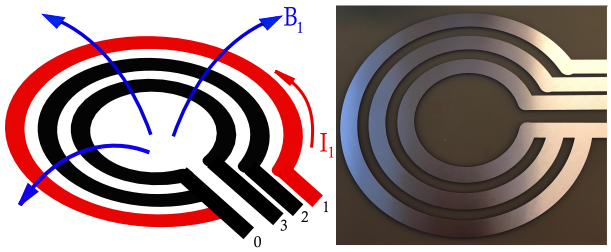

(a) (b)

Fig. 3. Three-loop switchable coil: (a) magnetic field representation when coil 1 is activated and coil 2-3 are short circuited; (b) fabricated coil on the PCB for measurements.

The mutual inductance $M_{12/13}$ between L_1 and $L_{2/3}$ is

$$M_{12/13} = \frac{\Phi_{2/3}}{I_1} = \frac{\mu_0 \pi r_{2/3}^2}{2r_1}. \quad (2)$$

In the same way mutual inductance M_{23} between coils L_2 and L_3 is calculated. Calculated mutual inductances, as well as self-inductance of each loop, are given in Table II.

TABLE II
CALCULATED SELF-INDUCTANCE AND MUTUAL INDUCTANCE

Loop n	Self-inductance L, nH	Mutual inductance		
		M_{12}, nH	M_{23}, nH	M_{13}, nH
1	378	108	71	55
2	271			
3	168			

D. Verification of the analysis

The three-loop switchable coil's structure is simulated in COMSOL Multiphysics, to verify calculation and measurement results. The inductor is also fabricated on the PCB as shown in Fig. 3(b). Measurement and simulation results comparison at 2 kHz is given in Table III. These values are comparable with the calculated results in Table II. One of the advantages of such coil design is a small parasitic resistance (in mΩ), which offers less ohmic losses. There is a difference between measurement and simulation results, which might be caused by an inaccuracy in the calibration of measurement equipment or errors in the fabrication process. It is worth mentioning that the estimated and simulated values are obtained with an assumption that the thickness of the copper layer is much smaller than the length and width of the coil.

TABLE III
SIMULATION AND MEASUREMENT RESULTS AT 2 KHZ

	Simulation			Measurement		
n[1]	L, nH	R, Ω	M, nH	L, nH	R, Ω	M, nH
1	361	0.036	M_{12} = 121	420	0.047	M_{12} = 155
2	274	0.023	M_{23} = 66	310	0.026	M_{23} = 81
3	196	0.014	M_{13} = 44	210	0.019	M_{13} = 50

[1] n – loop number

According to AC simulation results at 6.78 MHz (standard ISM band [10]) given in Table IV, there is a decrease in the self-inductance and mutual inductance due to parasitics such as the skin effect and parasitic capacitances.

TABLE IV
SIMULATED SELF-INDUCTANCE AND MUTUAL INDUCTANCE AT 6.78 MHZ

Loop n	Self-inductance L, nH	Mutual inductance		
		M_{12}, nH	M_{23}, nH	M_{13}, nH
1	324	116	65	45
2	220			
3	130			

III. MUTUAL INDUCTANCE BETWEEN SWITCHABLE COIL AND RESONANT COIL

The measurement and simulation results show that the estimation of the self-inductance and other parasitic components of the proposed coil is a straightforward process. Moreover, according to the simulation results, the impact of internal couplings between the loops on the self-inductance of the switchable coil is small. In this section, a relation between

TABLE V
PARAMETERS OF THE TEN-LOOP DRIVING COIL AND TRANSMITTER COIL

Parameter	Value	Unit	Description
n	1-10	–	index of the loop
r_n	1-10	cm	radius of the n-th loop
r_{out}	11.5	cm	outer radius of the spiral
r_{in}	1	cm	inner radius of the spiral
N	11	–	number of turns in the spiral
w	0.5	cm	width of loops
t	35	μm	thickness of the copper

the switchable driving coil L_V and a high Q resonating coil L_T on a two-sided PCB is measured, simulated and discussed.

The inductance of the switchable coil with three loops is limited in the range of 130-324 nH with three selections only. Therefore, the design of a switchable driving coil with ten loops is used in this section. The new version of the switchable inductor, as well as resonant coil design, are shown in Fig. 4. Here, the switchable driving coil consists of the ten loops, which are numbered 1 to 10 and located at the frontside of the PCB. The radius of the loops is varied from 1 to 10 cm. At the backside of the same PCB, a high-quality resonant coil with spiral shape can be seen, and its size and other parameters of the PCB are given in Table V.

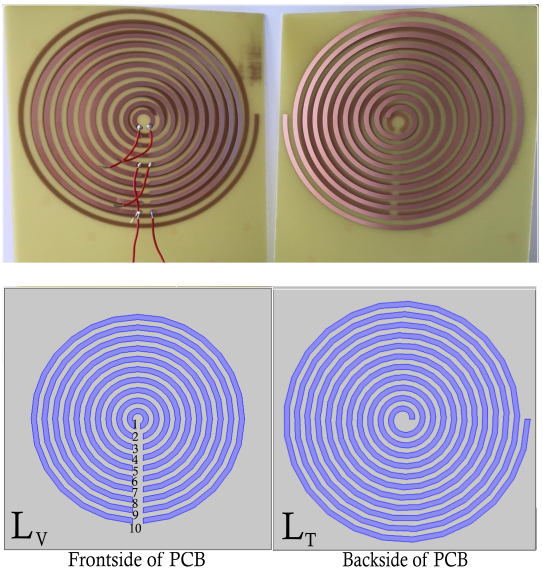

Fig. 4. Design of the switchable driving coil (frontside) and resonant coil (backside) on the PCB.

In order to derive the mutual inductance between driving coil L_V and resonating coil L_T, the self-inductance of each loop at 6.78 MHz is simulated via COMSOL Multiphysics which are given in Fig. 5. The almost perfect linearity of the mutual inductance can be noticed between loops 4 and 10. There is a non-linearity between loops 3 and 1, which, we think, is due to their position to the resonating coil. Nevertheless, the relative variation of the inductance from 19 nH to the 373 nH is achieved. Effect of the internal coupling on the self-inductance of the switchable driving coil is also

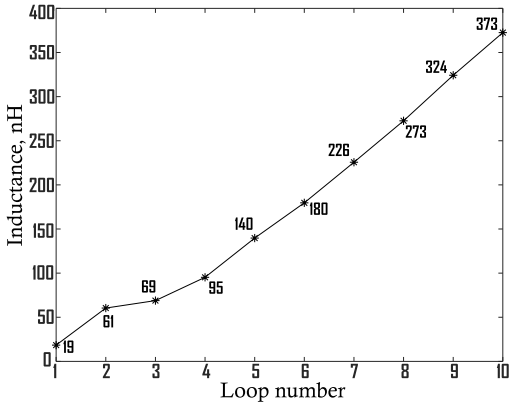

Fig. 5. Simulated self-inductances of the loops at 6.78 MHz.

tested, and it is again negligible. The self-inductance of the spiral coil is $L_T = 9.6$ μH.

Mutual inductance between the switchable driving coil L_V and resonator coil L_T versus frequency is shown in Fig. 6, where $M1$ represents the mutual inductance between loop 1 (the smallest) and L_T, whereas $M10$ - the mutual inductance between loop 10 (the outer) and L_T. The start frequency is 2 kHz. There is only a minor change of the mutual inductance over the simulated frequency range, which means the mutual inductance is not susceptible to the diversity of operating frequency.

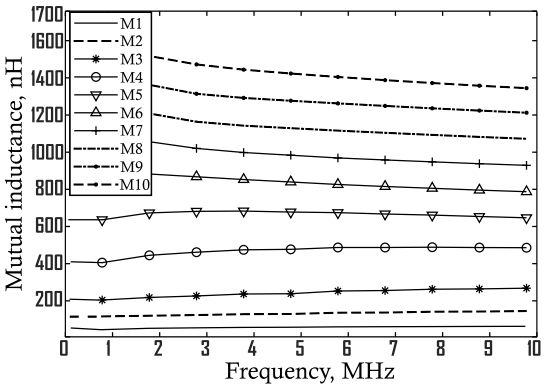

Fig. 6. AC simulation of the mutual inductance between the switchable driving coils L_V and the resonating coil L_T, where $M1$ is mutual inductance between loop 1 and L_T, $M2$ - loop 2 and L_T, $M3$ - loop 3 and L_T, $M4$ - loop 4 and L_T, $M5$ - loop 5 and L_T, $M6$ - loop 6 and L_T, $M7$ - loop 7 and L_T, $M8$ - loop 8 and L_T, $M9$ - loop 9 and L_T, $M10$ - loop 10 and L_T.

Finally, a comparison of simulated and measured values of mutual inductance and capacitance between the transmitter coil and the corresponding loop is shown in Figs. 7-8. Measurement has been obtained by using high precision GW-Intek LCR meter. Simulated values are represented by star sign and connected by a solid curve, whereas measured values are shown by plus sign and dashed curve. According to the measurements, mutual inductances are varied from 25 nH to 1230 nH, while the range of the capacitance is between 4.1 pF and 60.7 pF. Moreover, an almost linear behaviour

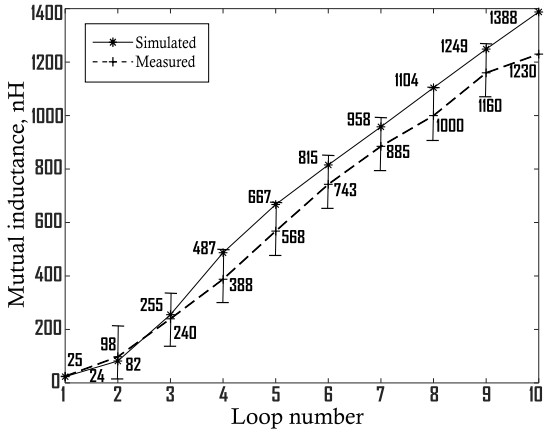

Fig. 7. Simulated and measured mutual inductance between the switchable driving L_V and resonant L_T coil at 2 kHz.

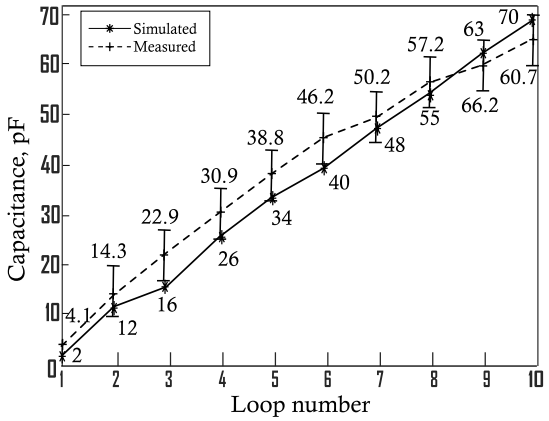

Fig. 8. Simulated and measured capacitance between switchable driving L_V and resonant L_T coils at 2 kHz.

of the trace can be seen for both parameters with a small deviation between simulation and measurement results. The deviation can be explained by parasitic components introduced by the measurement setup or inaccuracy during the fabrication process.

The inductance of the ten-loop switchable driving coil can be varied in the range from 19 nH to 373 nH at 6.78 MHz, which gives a better tunability compared to the three-loop model. There is also linearity in the change of mutual inductance between the switchable driving and resonant coils. Therefore, the switchable driving coil can be re-designed with many loops to achieve the desired range of the inductance variation at the different operating frequency. The linearity of the mutual inductance can be improved by more careful design of the coil parameters and increase the tuning range by driving several loops simultaneously. With this in mind, an extension of research will focus on performance analysis of the switchable driving coil in the inductive WPT system.

IV. Conclusion

The design of the switchable coil, where inductance can be controlled using switches, is studied. The structure of the coil is fabricated on the PCB with FR4 substrate. According to the simulation and measurement results of the three-loop coil, the internal couplings between the loops are minimum when one of the loop is active and others are short-circuited. The measurement results of the self-inductance and parasitic resistance of the coil correspond to the simulation and calculation. Measured parasitic resistance of the coil is 19-47 mΩ at 1 kHz. Three-loop switchable coil's inductance is varied between 130-324 nH at 6.78 MHz, which is a standard ISM band chosen by AirFuel Alliance.

An extended version of the switchable coil with ten loops together with a high Q-factor resonant coil is also analysed. In this case, the self-inductance of the switchable coil is varied from 19 nH to 373 nH at 6.78 MHz with an almost linear behaviour, whereas the inductance of the high-Q resonant coil is 9.6 μH. The simulation of mutual inductance between the switchable and the high-Q coils is verified by measurement results, which give an almost linear increase in the range of 25-1230 nH. The proposed switchable coil is a good candidate for driving and tuning high-quality resonators in MR WPT systems.

References

[1] A. P. Sample, D. A. Meyer, and J. R. Smith, "Analysis, experimental results, and range adaptation of magnetically coupled resonants for wireless power transfer", IEEE Trans. Ind. Electron., vol. 58, no. 2, pp. 544554, Feb. 2011.

[2] P. Park, C. S. Kim, M. Y. Park, S. D. Kim and H. K. Yu, "Variable inductance multilayer inductor with MOSFET switch control," in IEEE Electron Device Letters, vol. 25, no. 3, pp. 144-146, March 2004.

[3] B. K. Eplett, "On-chip impedance matching using a variable capacitor", U.S. Patent 2008/0211598 A1, Sep. 04, 2008.

[4] W. Lee, H. Lee, K. Oh, and J. Yu, "Switchable distance-based impedance matching networks for a tunable HF system", Progr. Electromagn. Res., vol. 128, pp. 1934, 2012.

[5] Y. Lim, H. Tang, S. Lim and J. Park, "An Adaptive Impedance-Matching Network Based on a Novel Capacitor Matrix for Wireless Power Transfer", in IEEE Transactions on Power Electronics, vol. 29, no. 8, pp. 4403-4413, Aug. 2014.

[6] J. Kim, D. H. Kim and Y. J. Park, "Analysis of Capacitive Impedance Matching Networks for Simultaneous Wireless Power Transfer to Multiple Devices", in IEEE Transactions on Industrial Electronics, vol. 62, no. 5, pp. 2807-2813, May 2015.

[7] A. Kurs, "Power transfer through strongly coupled resonances, Massachusetts Institute of Technology", Master Thesis, 2007.

[8] Y. Zhaksylyk, M. Azadmehr, "Comparative Analysis of Inductive and Capacitive feeding of Magnetic Resonance Wireless Power Transfer", IEEE PELS Workshop on Emerging Technologies: Wireless Power, 2018.

[9] S. S. Mohan, M. del Mar Hershenson, S. P. Boyd and T. H. Lee, "Simple accurate expressions for planar spiral inductances," in IEEE Journal of Solid-State Circuits, vol. 34, no. 10, pp. 1419-1424, Oct. 1999. doi: 10.1109/4.792620

[10] R. Tseng, B. von Novak, S. Shevde, and K. A. Grajski, Introduction to the Alliance for Wireless Power Loosely-Coupled Wireless Power Transfer System Specification Version 1.0, IEEE Wireless Power Transfer Conference, Perugia, Italy, May 2013.

[11] B. Park and J. Lee, "Adaptive Impedance Matching of Wireless Power Transmission Using Multi-Loop Feed With Single Operating Frequency," in IEEE Transactions on Antennas and Propagation, vol. 62, no. 5, pp. 2851-2856, May 2014. doi: 10.1109/TAP.2014.2307340

[12] Y. T. Song, J. J. Wang and X. M. Li, "Printed spiral coils with multiloop technique for planar magnetically coupled resonant wireless power transfer system," 2018 IEEE MTT-S International Wireless Symposium (IWS), Chengdu, 2018, pp. 1-3. doi: 10.1109/IEEE-IWS.2018.8400960